Supplementary Figure 1

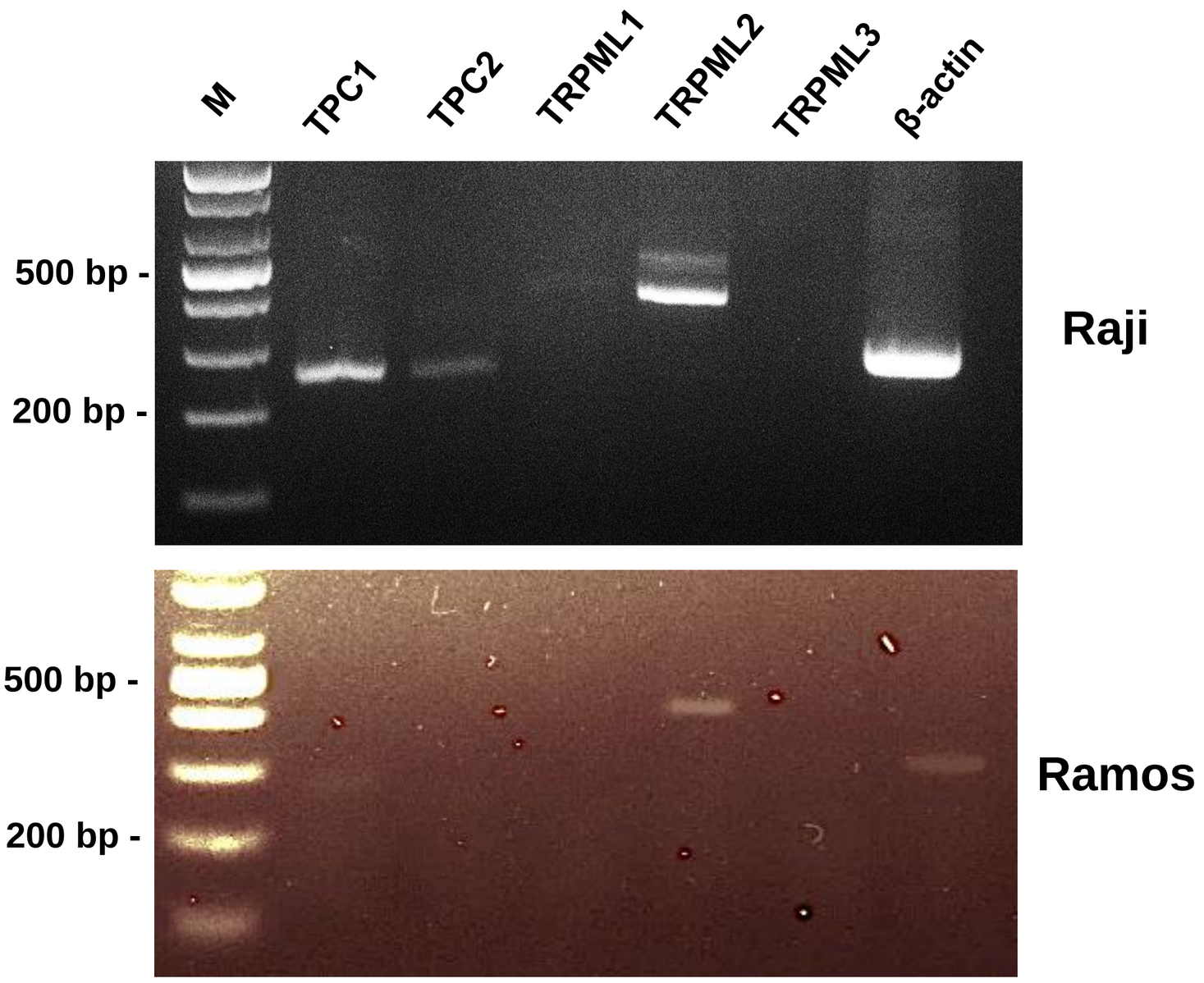

Supplementary Figure 1. Expression of lysosomal Ca^{2+} channel expressed in Raji cell and Ramos cell.
For Raji and Ramos cells, the lanes were as follows: M, DNA molecular weight markers; Lane 1, TPC1 (250 bp); Lane 2, TPC1 (250 bp); Lane 3, TRPML1 (409 bp); Lane 4, TRPML2 (504 bp); Lane 5, TRPML3 (579 bp); and Lane 6, β-actin (300 bp).

Supplementary Figure 2

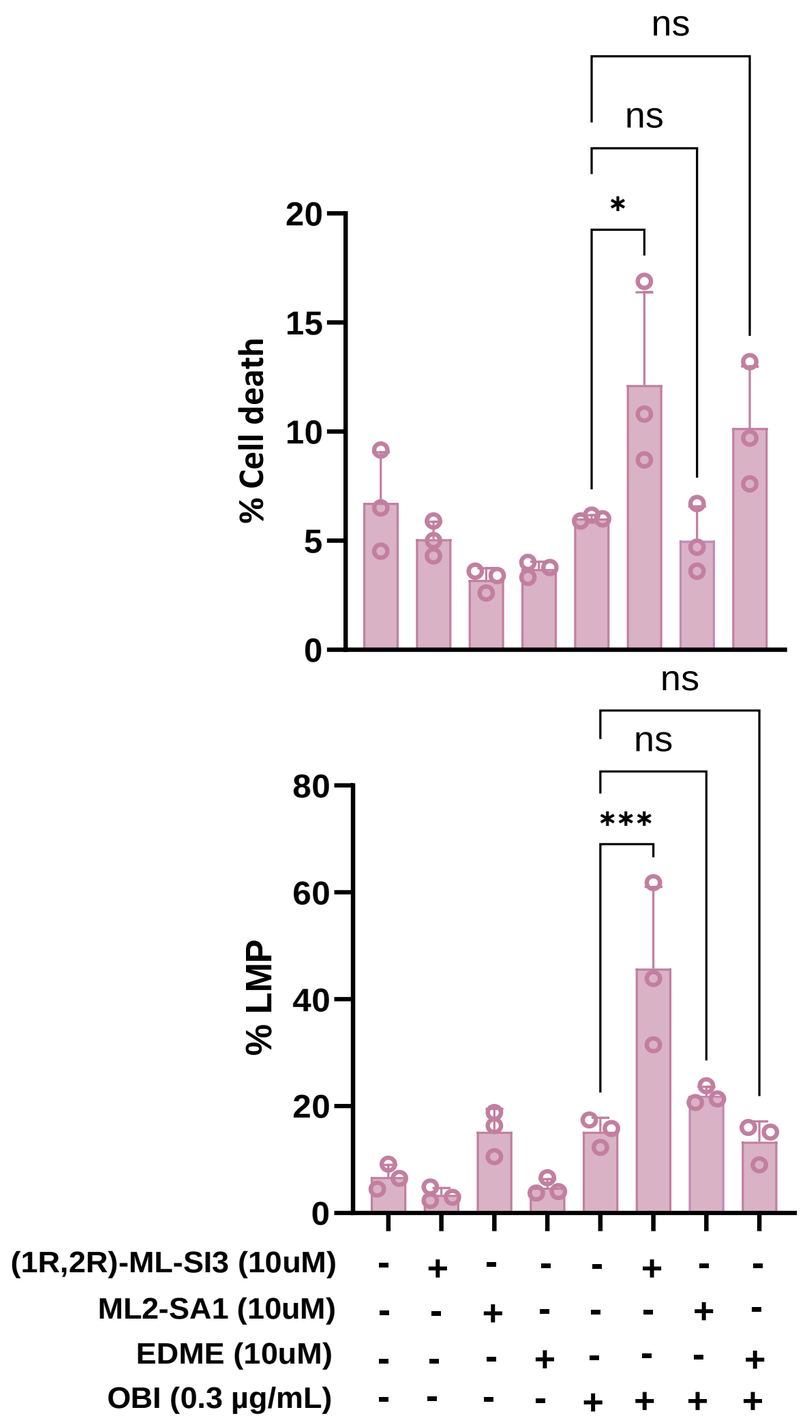

Supplementary Figure 2. Effects of TRPML modulators on cell death and lysosomal integrity in Raji cell

Effects of TRPML modulators on cell death and lysosomal integrity demonstrating TRPML2-specific contributions. Raji cells were pretreated with (1R,2R)-ML-SI3, ML2-SA1, or EDME for 2 h, followed by OBI exposure for an additional 2 h. LMP and DCD were quantified using LysoTracker Green and PI staining, respectively. Cells were treated with TRPML inhibitors or a TRPML2 activator, followed by assessment of cell death and lysosomal membrane permeabilization (LMP) using PI and LysoTracker green staining, demonstrating TRPML2-specific contributions.

Supplementary Figure 3

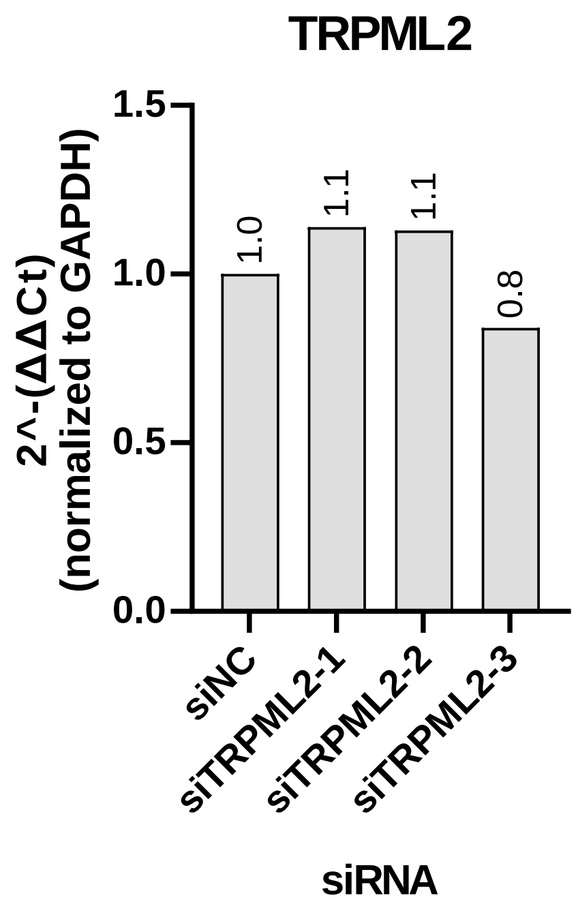

Supplementary Figure 3. Relative TRPML2 expression following siRNA-mediated knockdown in Raji
Relative TRPML2 expression in Raji cells transfected with three independent siRNAs targeting TRPML2 compared with negative control (NC) siRNA via qRT-PCR.

Supplementary Figure 4

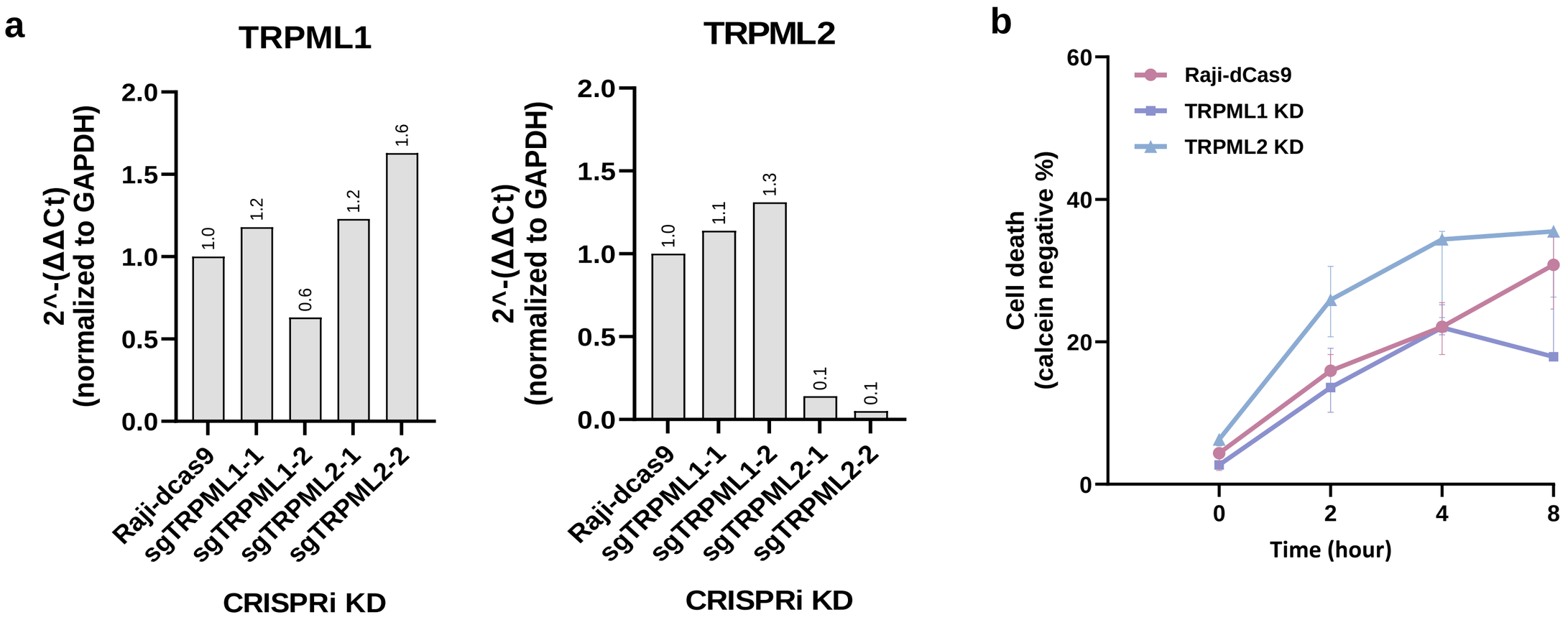

Supplementary Figure 4. Validation of TRPML1/2 knockdown efficiency and functional impact on Obinutuzumab-induced cytotoxicity in Raji cell

a. Quantitative RT-PCR analysis of TRPML1 and TRPML2 expression following CRISPR-mediated knockdown. Two independent sgRNAs were designed for each gene (sgTRPML1-1, sgTRPML1-2; sgTRPML2-1, sgTRPML2-2). Expression levels were normalized to GAPDH. **b** Cell death analysis of Raji cells transduced with sgTRPML1-2 or sgTRPML2-2 and treated with Obinutuzumab (0.3 μg/mL) in a time- and dose-dependent manner. TRPML2 knockdown cells exhibited enhanced cell death compared with Raji controls. Cell death was quantified at 2, 4, and 8 h post-treatment.

Supplementary Figure 5

a

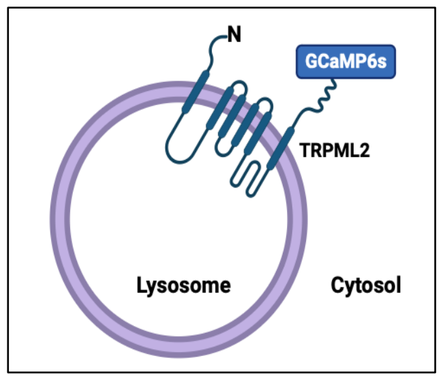

b

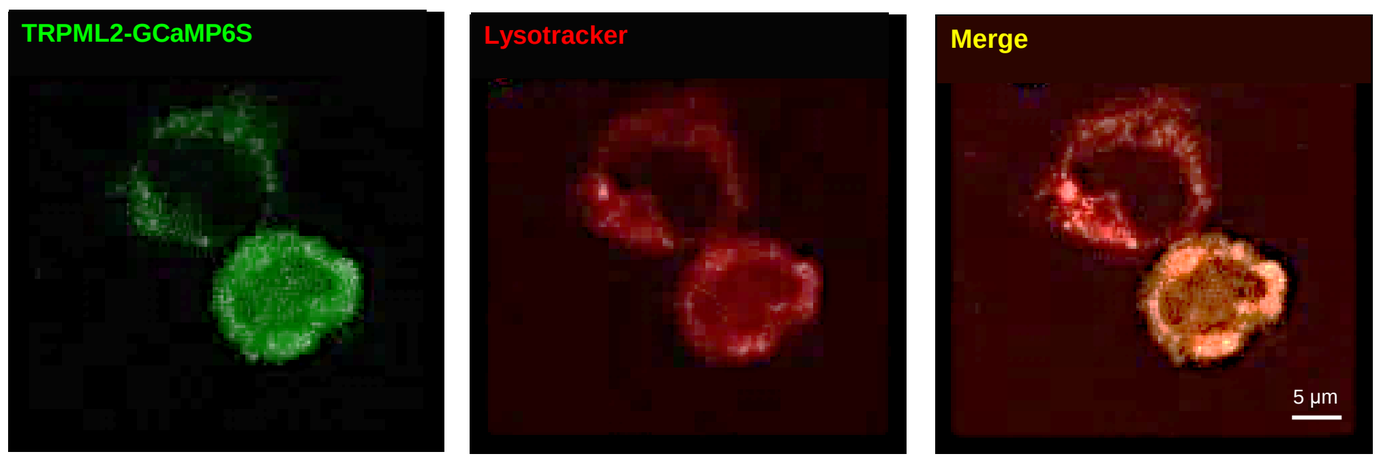

Supplementary Figure 5. The Construction scheme and proper localization of TRPML2-GCaMP6s. a. The construction scheme involved the fusion of GCaMP2 to the C-terminus of TRPML2 to enable Ca2+-dependent fluorescence signaling. **b.** TRPML2-GCaMP6S (green) and lysotracker red are co-localized in lysosome of Ramos cells.

Supplementary Figure 6

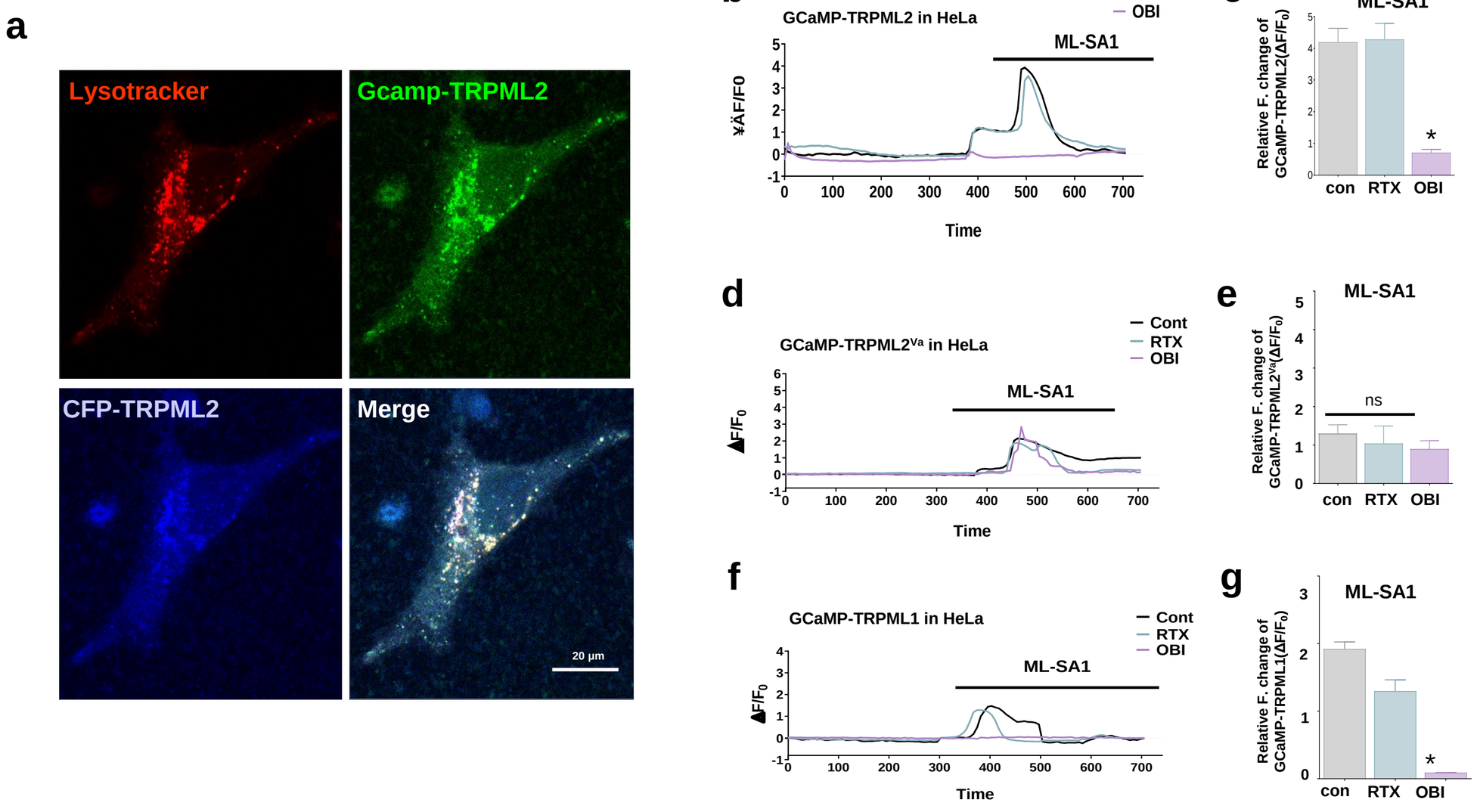

Supplementary Figure 6. Obinutuzumab inhibits ML-SA1 induced lysosomal Ca^{2+} release of TRPML2 and TRPML1 in HeLa cells overexpressed with CD20. a. GCaMP6S-TRPML2 localized in lysosome in HeLa cell. GCaMP6S-TRPML1 (green) and CFP-TRPML1 (blue) are well co-localized in Lysotracker (red) stained area. Evaluation of OBI's effect on TRPML2 activity in HeLa cells using fluorescence changes of TRPML2-GCaMP6S **(b,c),** GCaMP6s-TRPML2^{Va} **(d,e)** and TRPML1-GCaMP6S **(f,g).** Antibodies treated at starts and then treated with 20 μM ML-SA1 **(b, d, f)** at indicated point. Summary ML-SA1-induced **(c, e, g)** Ca^{2+} release in control, rituximab and obinutuzumab treatment in Hela cells.

Supplementary Figure 7

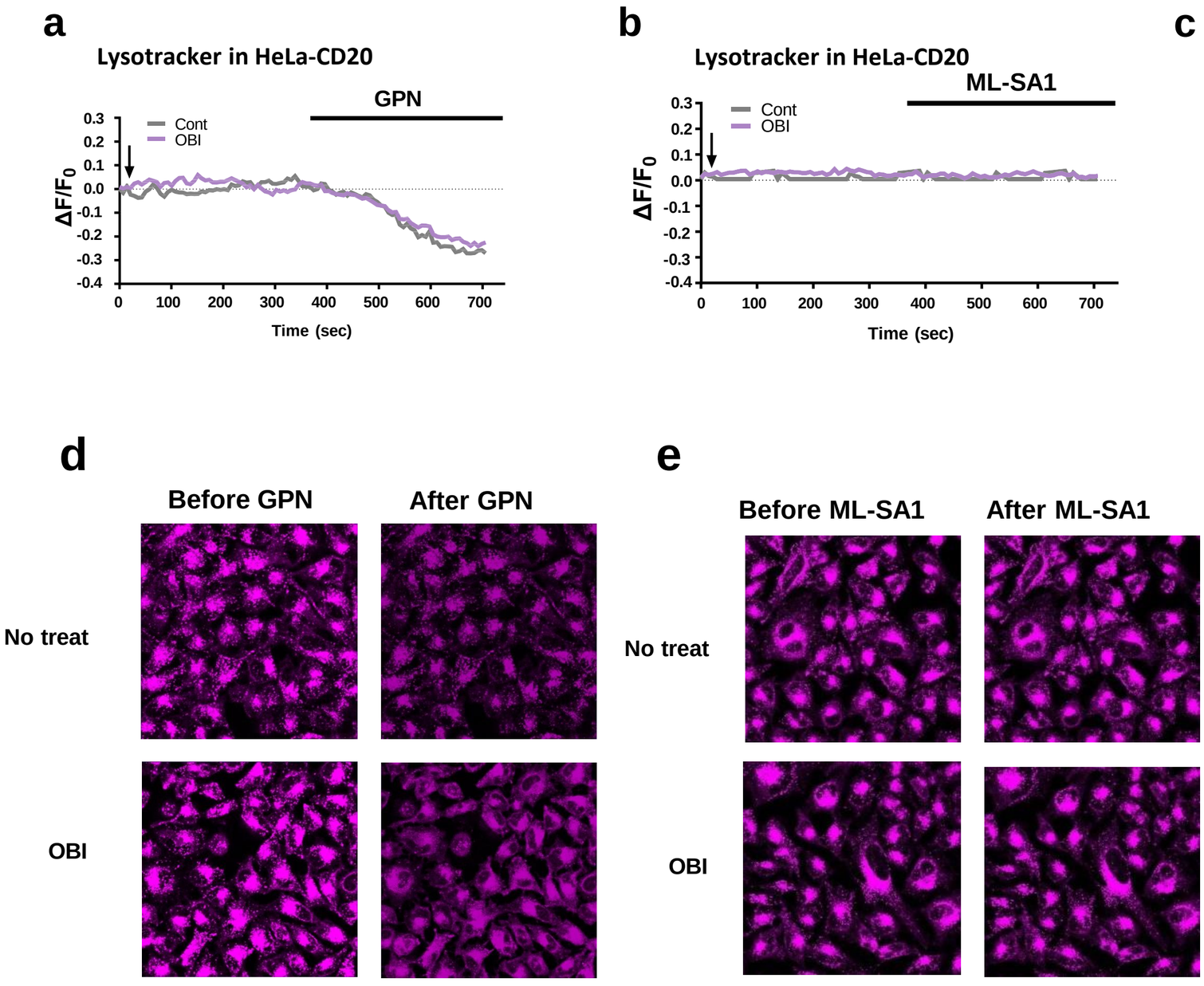

Supplementary Figure 7. Intact lysosomes during OBI treatment and up to the time of TRPML2 inhibition. Representative traces and images of Lysotracker far red staining the acidic vesicles in CD20 expressing HeLa cells to confirm the lysosome integrity. Mock or OBI was treated at the beginning and GPN **(a, d)** or ML-SA1 **(b, e)** was treated at indicated point. **c.** Average GPN-induced or ML-SA1-induced fluorescence change of Lysotracker in control, OBI treatment in HeLa cells.

Supplementary Figure 8

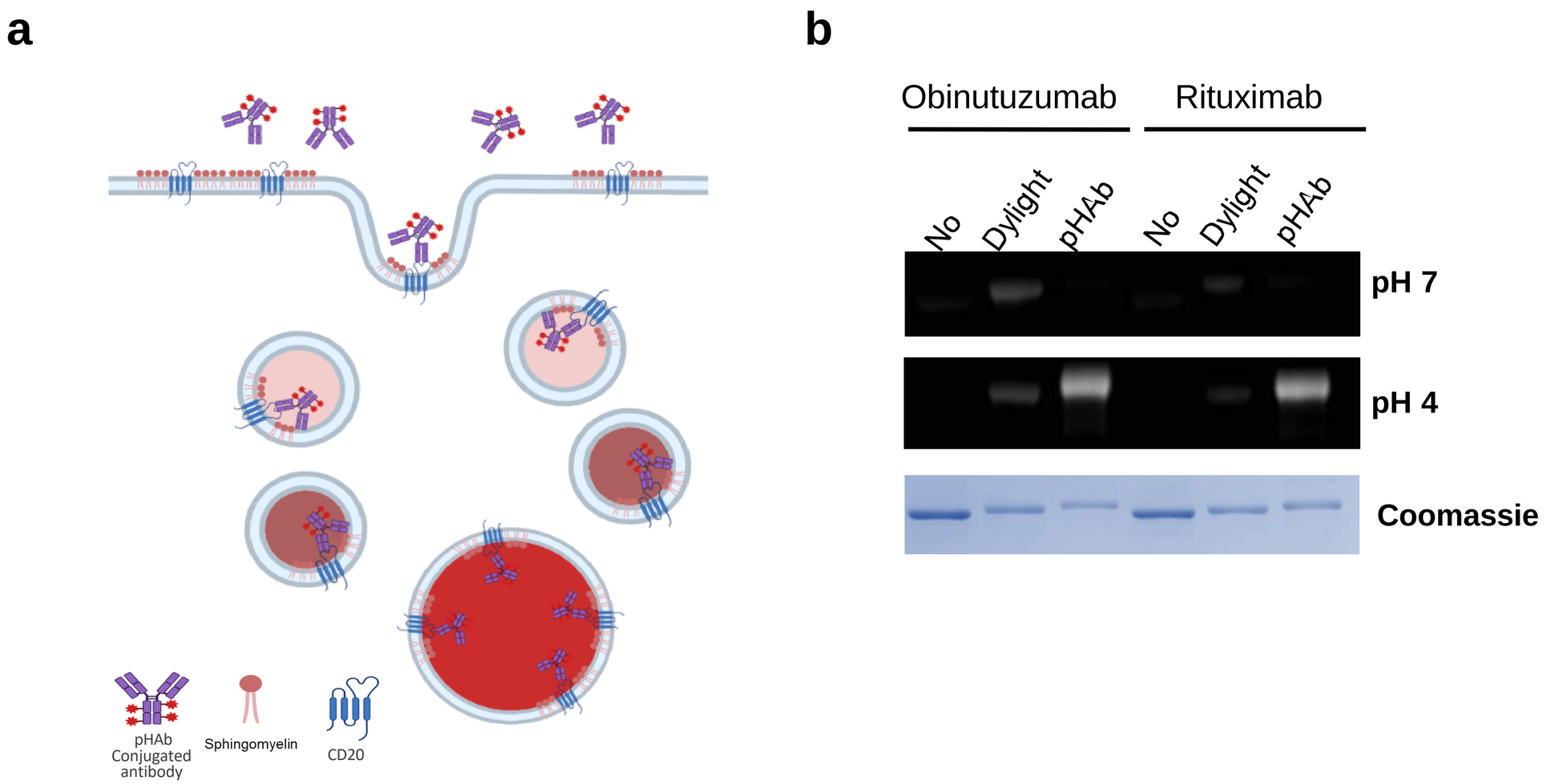

Supplementary Figure 8. Endocytosis of obinutuzumab monitored by pHAb labeling **a.** Schematic diagram illustrating endocytosis process of pHAb-conjugated antibody. **b.** SDS-PAGE image of obinutuzumab-pHAb and rituximab-pHAb in pH 3.0 or pH 7.0 condition compared with Dylight-conjugated antibodies. The equal amount of each antibody was confirmed by coomassie staining.

Supplementary Figure 9

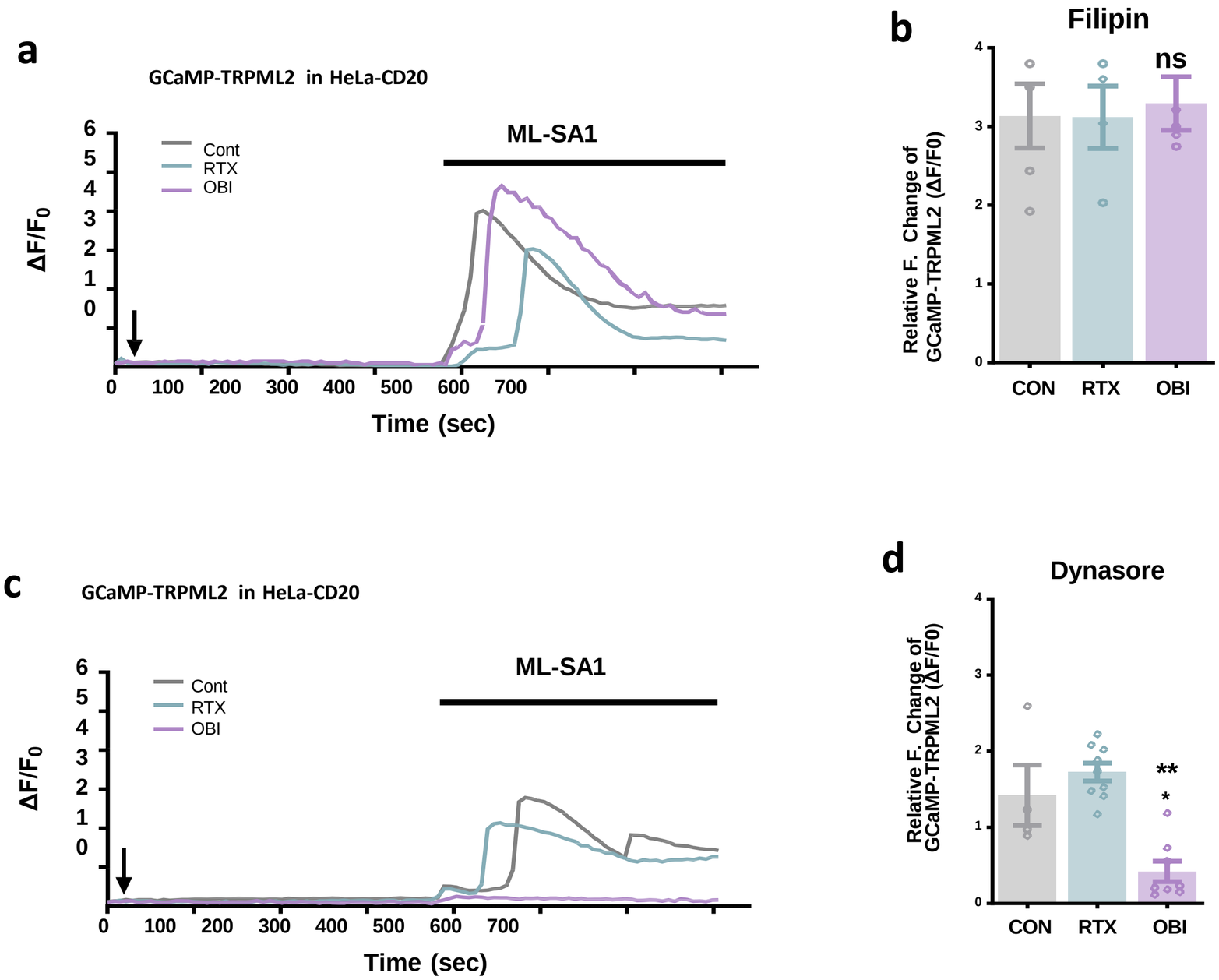

Supplementary Figure 9. Filipin reversed the obinutuzumab inhibition of TRPML2 in CD20 stable expressing HeLa cells a-d. Mean GCaMP6S- TRPML2 fluorescence traces of filipin-pretreated (**a**) or dynasore-pretreated (**c**) CD20-expressing HeLa cells treated with antibodies at starts and then treated ML-SA1 at indicated point. Average ML-SA1 induced Ca^{2+} release in control, rituximab, and obinutuzumab treated cells after filipin (**b**) and dynasore (**d**) pretreatment. Data are presented as the mean ± SEM. Statistical comparisons were made by using variance analysis. *$p < 0.05$ vs. control.

Supplementary Figure 10

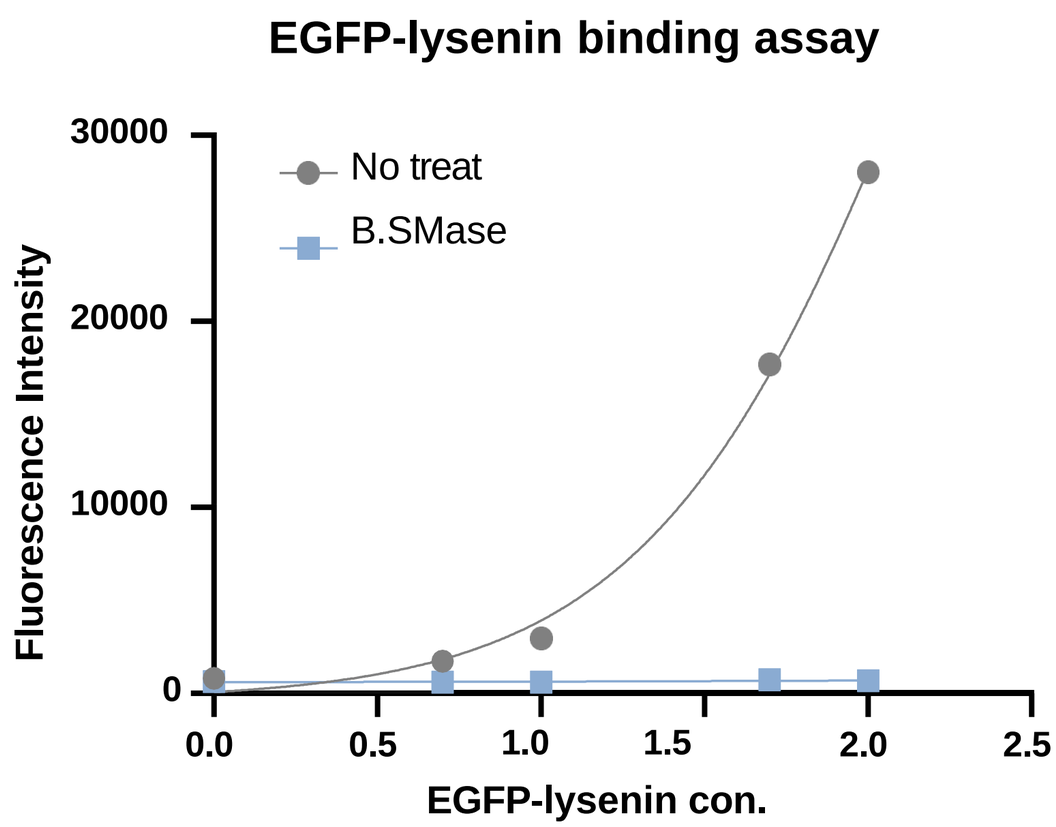

Supplementary Figure 10. Sphingomyelin depletion by bacterial sphingomyelinase confirmed via EGFP-lysenin binding. Raji cell treated with or without bacterial sphingomyelinase were treated with each concentration of GFP-lysenin then measured GFP fluorescence by FACS. GFP-lysenin amount dependent increased fluorescence was not observed in bacterial sphingomyelinase treated cells.